An NMR Analysis of Ubiquitin Recognition by Yeast Ubiquitin Hydrolase: Evidence for Novel Substrate Recognition by a Cysteine Protease†

Taiichi Sakamoto,‡ Takeshi Tanaka,‡ Yutaka Ito,§ Sundaresan Rajesh,§,|| Mariko Iwamoto-Sugai,‡ Yoshio Kodera,‡,⊥ Nobuo Tsuchida,|| Takehiko Shibata,§ and Toshiyuki Kohno*,‡

Mitsubishi Kasei Institute of Life Sciences, Machida, Tokyo 194-8511, Japan, Laboratory of Cellular and Molecular Biology, The Institute of Physical and Chemical Research (RIKEN), Wako, Saitama 351-0198, Japan, Laboratory of Molecular Cellular Oncology, Tokyo Medical and Dental University, Bunkyo, Tokyo 113-8549, Japan, and Department of Physics, School of Science, Kitasato University, Sagamihara, Kanagawa 228-8555, Japan

Received February 9, 1999; Revised Manuscript Received June 21, 1999

ABSTRACT: Yeast ubiquitin hydrolase 1 (YUH1), a cysteine protease that catalyzes the removal of ubiquitin C-terminal adducts, is important for the generation of monomeric ubiquitin. Heteronuclear NMR spectroscopy has been utilized to map the YUH1 binding surface on ubiquitin. When YUH1 was titrated into a sample of ubiquitin, approximately 50% of the $^{1}H-^{15}N$ correlation peaks of ubiquitin were affected to some degree, as a result of binding to YUH1. It is noteworthy that the amide resonances of the basic residues (Arg42, Lys48, Arg72, and Lys74) were highly perturbed. These positively charged basic residues may be involved in direct interactions with the negatively charged acidic residues on YUH1. In addition to the electrostatic surface, the hydrophobic surfaces on ubiquitin (Leu8, Ile44, Phe45, Val70, Leu71, and Leu73) and YUH1 are also likely to contribute to the binding interaction. Furthermore, the amide resonances of Ile13, Leu43, Leu50, and Leu69, the side chains of which are not on the surface, were also highly perturbed, indicating substrate-induced changes in the environments of these residues as well. These large changes, observed from residues located throughout the five-stranded β-sheet surface and the C-terminus, suggest that substrate recognition by YUH1 involves a wider area on ubiquitin.

Ubiquitin is a small (8.6 kDa, Figure 1), highly conserved protein distributed universally among eukaryotes (for reviews see refs *1*−*4*). It has been implicated in numerous cellular processes, including cell cycle control, apoptosis, regulation of transcription, stress responses, maintenance of chromatin structure, DNA repair, signal transduction, and antigen presentation. Many ubiquitin-dependent pathways involve progressive degradation of ubiquitin-conjugated proteins by the 26S proteasome complex.

The coupling of ubiquitin to other proteins is catalyzed by a family of ubiquitin-conjugating enzymes and involves the formation of an isopeptide bond between the C-terminal Gly residue of ubiquitin and the ϵ-amino group of a Lys residue in the target protein. Alternatively, the target protein can be polyubiquitinated, with a Lys residue of the first ubiquitin conjugated to the C-terminus of the next. Efficient targeting for degradation by the 26S protease appears to require polyubiquitination (*5*, *6*). Following degradation, the ubiquitin isopeptide bond is hydrolyzed by deubiquitinating enzymes (for reviews see ref *7*). This hydrolysis is essential to recycle ubiquitin for further conjugation as well as to prevent the accumulation of polyubiquitin chains, which are known to bind the 26S proteasome and to inhibit degradation.

In addition to the isopeptide bond, deubiquitinating enzymes hydrolyze α-linked peptide bonds to generate ubiquitin from its precursor, since all known ubiquitin genes encode polyubiquitin or fusion proteins in which ubiquitin is followed by a ribosomal protein (*8*). The proubiquitin gene product consists of multiple copies of ubiquitin, is induced by stress, and must be processed to monomeric ubiquitin by deubiquitinating enzymes. Similarly, ubiquitin−ribosomal protein fusions, synthesized in rapidly growing cells, must be accurately processed to release the ubiquitin and ribosomal proteins.

Deubiquitinating enzymes fall into two distinct families of cysteine proteases, *ub*iquitin-specific *p*roteases (UBPs)[1] (*9*, *10*) and *u*biquitin *c*-terminal *h*ydrolases (UCHs) (*11*). The UBP enzymes were named for their ability to cleave large model fusion proteins at the C-terminus of ubiquitin. They vary in molecular mass from 50 to 300 kDa and exhibit a broad range of substrate specificity. Roles assigned for UBPs include the cleavage of ubiquitin from the remnants of a degraded protein (*12*) and the disassembly of polyubiquitin

† This work was supported in part by grants for the Biodesign Research Program and the MR Sciences from RIKEN to Y.I.

* To whom correspondence should be addressed. Tel: +81-42-724-6285. Fax: +81-42-724-6317. E-mail: tkohno@libra.ls.m-kagaku.co.jp.

‡ Mitsubishi Kasei Institute of Life Sciences.

§ The Institute of Physical and Chemical Research (RIKEN).

|| Tokyo Medical and Dental University.

⊥ Kitasato University.

[1] Abbreviations: CSI, chemical shift index; DSS, 4,4-dimethyl-4-silapentane-1-sulfonic acid; DTT, dithiothreitol; *E. coli*, *Escherichia coli*; HSQC, heteronuclear single-quantum coherence; IPTG, isopropyl β-D(−)-thiogalactopyranoside; NMR, nuclear magnetic resonance; NOESY, nuclear Overhauser effect spectroscopy; PCR, polymerase chain reaction; *S. cerevisiae*, *Saccharomyces cerevisiae;* SDS−PAGE, sodium dodecyl sulfate−polyacrylamide gel electrophoresis; TOCSY, total correlation spectroscopy; TOF-MS, time-of-flight mass spectroscopy; TPPI, time-proportional phase increment; UBPs, ubiquitin-specific proteases; UCHs, ubiquitin C-terminal hydrolases; WATERGATE, water suppression by gradient-tailored excitation; YUH1, yeast ubiquitin hydrolase 1. Standard abbreviations are used for usual amino acids.

10.1021/bi990310y CCC: $18.00
Published on Web 08/19/1999

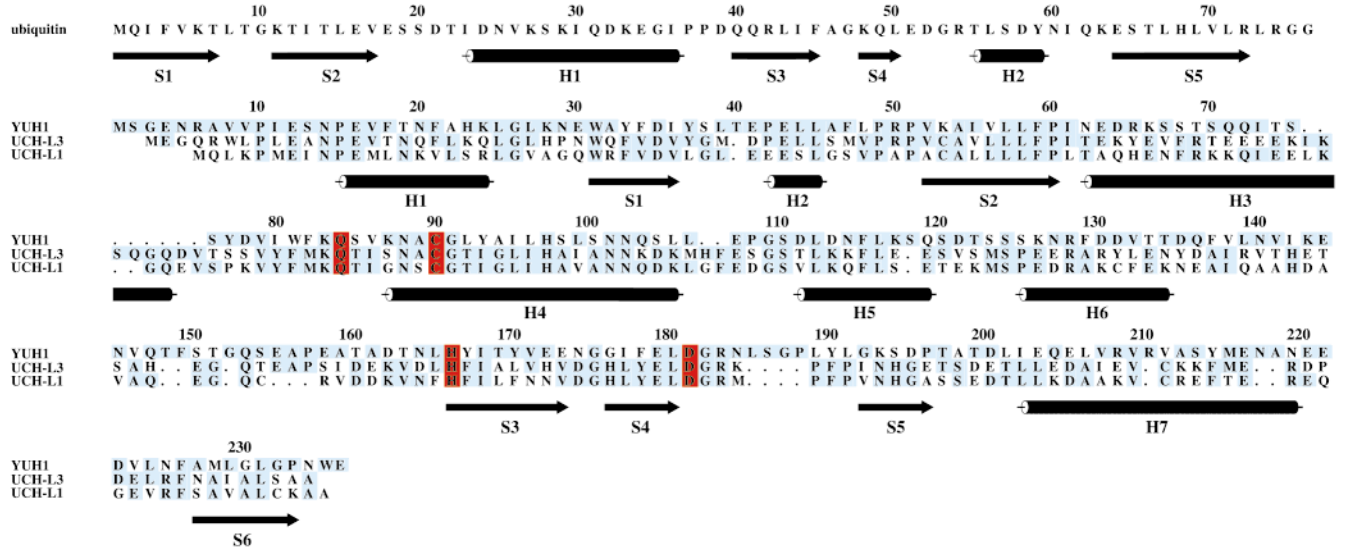

FIGURE 1: Sequence of yeast ubiquitin and sequence alignment of UCH enzymes. Secondary structural elements seen in the ubiquitin and UCH-L3 structure are indicated below the sequences, according to the reported tertiary structures (*18, 51*). Possible active site residues (Gln84, Cys90, His166, and Asp181) of YUH1 are indicated in red. The program ALSCRIPT (*61*) was used to display the sequence alignment.

chains to yield functional monomers (*4*). They appear to function in cell fate determination (*13*), transcriptional silencing (*14, 15*), and the responses to cytokines (*16*).

The UCH enzymes are generally smaller (25−28 kDa) than the UBPs. The yeast ubiquitin hydrolase (YUH1; 26 kDa) used in this study belongs to the UCH family (*17*). Disruption or deletion of the YUH1 gene confers no discernible phenotype, suggesting that the substrate specificity of the UCH enzymes may overlap with that of the UBP enzymes (*10, 17*). Biochemical studies have demonstrated that YUH1, the human enzymes UCH-L1 and UCH-L3, and the UCH from *Drosophila melanogaster* hydrolyze α- and ϵ-linked amide bonds at the C-terminus of ubiquitin, although most studies have focused on the hydrolysis of α-linked peptide bonds and small thioester-, ester-, and amide-linked adducts (*11, 18*−*21*). In general, most of these small adducts are good substrates, except for peptide extensions with proline immediately following the scissile bond. The YUH1 protein is known to cleave mainly short ubiquitin conjugates and is used to prepare short peptides in an *Escherichia coli* expression system (*17, 22, 23*). UCH-L3 also cleaves peptide extensions of up to 20 residues from ubiquitin with high efficiency and low sequence preference, while larger folded extensions are not cleaved (*7, 21*). These data suggest that the UCH enzymes may function to regenerate active ubiquitin from adducts with small nucleophiles (*11, 21*).

Recently, Johnston et al. have determined the crystal structure of UCH-L3, which has 30% sequence identity to YUH1 (Figure 1) (*18*). Site-directed mutagenesis of the invariant residues on UCH-L1 implicated Cys90 (YUH1 numbering) as the active site nucleophile and His166 as the general base in catalysis, with an important role also played by Asp181 (*24*), and these residues are conserved among the members of the UCH family. A model of the complex between UCH-L3 and ubiquitin was proposed from computer modeling on the basis of the structure of UCH-L3 alone. However, direct information about the residues of ubiquitin recognized by the UCH family of proteases has not been reported yet. To understand the recognition mechanism of ubiquitin by the UCH cysteine protease, we performed NMR analyses on ubiquitin and observed the chemical shift changes of the backbone resonances upon YUH1 binding.

MATERIALS AND METHODS

Materials. The following materials were used: pET vectors (Novagen, Madison, WI), DEAE Sepharose FF, SP Sepharose FF, HiLoad 26/60 Superdex (75 pg), and RESOURCE Q (6 mL) (Pharmacia Biotech, Tokyo, Japan), and ^2H_2O, [^{15}N]ammonium chloride (99% ^{15}N), and [$^{13}C_6$]-D-glucose (ISOTEC Inc., Miamisburg, OH). All other reagents were of analytical grade (Nacalai Tesque, Kyoto, Japan).

Preparation of YUH1. The gene encoding YUH1 was cloned by the method described (*23*) and was ligated into the *Nde*I/*Sal* I sites of the pET-24a vector, to produce pET-24a/YUH1. *E. coli* BL21(DE3) cells harboring the plasmid encoding YUH1 (pET-24a/YUH1) were cultured at 37 °C overnight in 5 mL of LB medium containing 50 μg/mL kanamycin and then were transferred to 2 L of the same medium. When the OD_{600} reached 1.0, IPTG (0.1 mM) was added, and protein expression was induced for 12 h at 37 °C. The cells were harvested, dispersed in 200 mL of buffer A containing 50 mM Tris-HCl (pH 8.0) and 2 mM DTT, and then disrupted using 20 mg of hen egg lysozyme and 15 min of sonication. After centrifugation, the supernatant was loaded onto a 100 mL column of DEAE Sepharose FF equilibrated with buffer A. Following a wash step with 500 mL of buffer A, the YUH1 protein was eluted by an NaCl gradient from 0 to 500 mM in buffer A (900 mL). The YUH1 protein was eluted at about 300 mM NaCl, and the fractions containing YUH1 were concentrated to 10 mL with a Centriprep-10 unit (Amicon, Beverly, MA). The concentrated YUH1 protein was loaded onto a HiLoad 26/60 Superdex 75 pg column equilibrated with buffer A. The fractions containing YUH1 were loaded onto a RESOURCE Q (6 mL) column equilibrated with the buffer A using an FPLC system (Pharmacia Biotech, Tokyo, Japan). Following a wash step with 30 mL of buffer A, YUH1 was eluted by an NaCl

gradient from 0 to 400 mM in buffer A (30 mL). The YUH1 protein was eluted at about 300 mM NaCl, and its purity was confirmed by SDS−PAGE. Using Centriprep-10 and Centricon-10 units (Amicon, Beverly, MA), the buffer of the fractions containing YUH1 was exchanged with NMR sample buffer [50 mM sodium phosphate (pH 6.0), 100 mM NaCl, 5 mM DTT, 1 mM DSS, 10% ^2H_2O], and the YUH1 protein was concentrated to 7.6 mM. Protein concentrations were determined by the Bio-Rad Protein Assay (Bio-Rad, Tokyo, Japan) with BSA as the standard.

Preparation of Ubiquitin. The gene encoding ubiquitin was cloned by the method described (*23*) and was ligated into the *Nde*I/*Sal*I sites of the pET-24a vector, to produce pET-24a/ubiquitin. *E. coli* BL21(DE3) cells harboring the plasmid encoding ubiquitin (pET-24a/ubiquitin) were cultured at 37 °C overnight in 5 mL of LB medium containing 50 μg/mL kanamycin and then were transferred to 2 L of M9 minimal medium supplemented with trace elements and $^{15}NH_4Cl$ (1 g/L), as described (*23*, *25*, *26*). When the OD_{600} reached 1.0, IPTG (final 0.1 mM) was added, and protein expression was induced for 12 h at 37 °C. The uniformly $^{13}C/^{15}N$-labeled ubiquitin was prepared under the same conditions as those used for the uniform ^{15}N-labeling, except for the use of [$^{13}C_6$]-D-glucose (1 g/L) and $^{15}NH_4Cl$ (1 g/L). The uniformly 50% $^2H/^{13}C/^{15}N$-labeled ubiquitin was prepared under the same conditions as those used for the uniform ^{15}N-labeling, except for the use of [$^{13}C_6$]-D-glucose (1 g/L), $^{15}NH_4Cl$ (1 g/L), and ^2H_2O (60%). The cells were harvested, dispersed in 100 mL of buffer B containing 50 mM sodium acetate (pH 5.0) and 2 mM DTT, and then disrupted using 10 mg of hen egg lysozyme and 15 min of sonication. After centrifugation, the supernatant was incubated at 85 °C for 5 min and chilled on ice. After a further centrifugation step, the supernatant was loaded onto a 25 mL column of SP Sepharose FF equilibrated with buffer B. Following a wash step with 100 mL of buffer B, the ubiquitin was eluted by an NaCl gradient from 0 to 500 mM in buffer B (200 mL). The ubiquitin was eluted at about 150 mM NaCl. The fractions containing ubiquitin were lyophilized and redissolved in 10 mL of buffer A, as described above. After centrifugation, the supernatant was loaded onto a HiLoad 26/60 Superdex 75 pg column equilibrated with buffer A. The fractions containing ubiquitin were dialyzed twice against 2 L of deionized water and lyophilized.

IAsys Optical Biosenser Measurements. Experiments were performed using an IAsys resonant mirror optical biosensor (Affinity Sensors, Cambridge, U.K.). Ubiquitin was immobilized on (carboxymethyl)dextran cuvette surfaces according to the manufacturer's instructions. Binding experiments were performed in 50 mM sodium phosphate and 100 mM sodium chloride, pH 6.0. YUH1 was added to a final concentration of 1, 2.5, 5, 10, and 20 μM in a total volume of 50 μL, respectively. Changes in resonant angle were monitored at 1-s intervals for approximately 300 s. Experiments were performed at 25 °C with a stirrer speed of 100 rpm. For repeated measurements using the same cuvette, surfaces were regenerated by washing for 2 min in 10 mM acetic acid.

NMR Analyses. NMR samples contained approximately 2 mM ubiquitin in NMR sample buffer [50 mM sodium phosphate (pH 6.0), 100 mM NaCl, 5 mM DTT, 1 mM DSS, 10% ^2H_2O]. All NMR measurements were performed on either a Bruker AMX-500 or DRX-600 spectrometer at 30 °C. To assign the backbone resonances of ubiquitin in the absence of YUH1, $^{13}C/^{15}N$-enriched ubiquitin was used to measure the 2D HSQC, 3D CBCA(CO)NNH (*27*−*29*), and 3D HNCACB (*28*−*30*) spectra. The 2D HSQC spectra were acquired with 256 (t_1) × 1024 (t_2) complex points. Both of the 3D spectra were acquired with 32 (t_1) × 32 (t_2) × 512 (t_3) complex points. The 2D HSQC titrations were carried out by adding concentrated YUH1 (7.6 mM), dissolved in the same NMR sample buffer, to ^{15}N-enriched ubiquitin. For the assignment of the backbone resonances of ubiquitin bound to YUH1, the uniformly 50% $^2H/^{13}C/^{15}N$/-labeled ubiquitin complexed with YUH1 (1:1.1; approximately 2 mM) was used to record the 3D HNCA (*31*) and 3D HN(CO)CA (*32*) spectra. These triple-resonance spectra were acquired with a total of 64 (t_1) × 32 (t_2) × 512 (t_3) complex points, with constant-time evolution periods for both ^{13}C and ^{15}N dimensions and with ^2H decoupling. For all NMR experiments, the water resonance was suppressed by using the WATERGATE scheme (*33*) and water flip-back pulses (*34*).

Data processing was performed on a Bruker X-32 UNIX workstation with UXNMR software, on a Silicon Graphics O2 workstation using the program package NMRPipe (*35*) or on a Silicon Graphics Indigo^2 workstation using the Azara software package (Boucher, unpublished). For the 3D NMR data sets, the linear prediction method (*36*, *37*) from the NMRpipe package or the 2D maximum entropy method from the Azara package was employed to extend the data in the indirectly acquired dimensions. All of the spectra were analyzed with a combination of customized macroprograms from the Ansig version 3.3 software (*38*, *39*).

The ^1H and ^{13}C shifts were referenced to the methyl resonance of 4,4-dimethyl-4-silapentane-1-sulfonic acid (DSS), used as an internal standard. The ^{15}N chemical shifts were indirectly referenced using the ratio (0.101329118) of the zero-point frequencies to ^1H (*40*). For structural analyses, the coordinates of human ubiquitin were obtained from the Brookhaven Protein Data Bank, entry 1UBI.

RESULTS AND DISCUSSION

NMR Resonance Assignments of Ubiquitin. The amide proton resonances are well dispersed in the $^1H-^{15}N$ HSQC spectrum of ^{15}N-enriched ubiquitin. Therefore, the assignments of the amide (N and HN) resonances in the absence of YUH1 were based mainly on the 3D ^{15}N-edited TOCSY−HSQC and 3D ^{15}N-edited NOESY−HSQC spectra. The assignment of the amide resonances was then confirmed on the basis of the 3D CBCACONH and 3D HNCACB experiments (Table 1). The $^1H-^{15}N$ HSQC spectrum of ubiquitin in the absence of YUH1, with the complete amide resonance assignments, is shown in Figure 2a. Yeast ubiquitin differs from human ubiquitin by only three residues. The differences between yeast and human ubiquitin are as follows: Ser19 to Pro19, Asp24 to Glu24, and Ser28 to Ala28, respectively. The chemical shifts of the amide resonances of yeast ubiquitin were very similar to those reported for human ubiquitin (*41*), except for these three amino acid residues, suggesting that the structure of yeast ubiquitin is similar to that of human ubiquitin. In fact, it was reported that the structure of yeast ubiquitin is quite similar to that of human ubiquitin on the basis of difference

Table 1: ^{1}H, ^{15}N, and ^{13}C Chemical Shifts for Ubiquitin at 30 °C, pH 6.0

	ubiquitin in the absence of YUH1				ubiquitin bound to YUH1				ubiquitin in the absence of YUH1				ubiquitin bound to YUH1		
	^{15}N	NH	$^{13}C^{\alpha}$	$^{13}C^{\beta}$	^{15}N	NH	$^{13}C^{\alpha}$		^{15}N	NH	$^{13}C^{\alpha}$	$^{13}C^{\beta}$	^{15}N	NH	$^{13}C^{\alpha}$
Met[1]			54.49	33.15			54.07	Asp[39]	114.10	8.47	55.66	39.68	114.61	8.49	55.46
Gln[2]	123.50	8.88	55.03	30.51	123.77	8.90	54.61	Gln[40]	117.57	7.80	55.52	30.05	117.67	7.63	55.33
Ile[3]	115.90	8.29	59.46	42.01	115.94	8.22	59.12	Gln[41]	118.72	7.45	56.49	31.45	117.75	7.43	55.97
Phe[4]	119.28	8.56	55.05	41.07	119.21	8.44	54.72	Arg[42]	123.71	8.49	54.99	31.60	nd	nd	nd
Val[5]	121.98	9.26	60.36	34.09	122.79	9.34	60.19	Leu[43]	125.00	8.76	52.92	45.58	nd	nd	nd
Lys[6]	128.61	8.91	54.52	34.40	128.47	8.77	54.05	Ile[44]	122.99	9.07	58.87	41.11	nd	nd	nd
Thr[7]	116.06	8.70	60.39	30.67	nd[a]	nd	nd	Phe[45]	125.73	8.81	56.46	43.56	nd	nd	nd
Leu[8]	121.96	9.04	57.41	41.85	121.61	8.91	nd	Ala[46]	133.42	8.91	52.44	56.72	nd	nd	nd
Thr[9]	106.48	7.61	61.38	29.43	104.59	7.59	61.33	Gly[47]	103.17	8.07	45.25		102.47	7.66	
Gly[10]	109.88	7.79	45.26		109.98	7.88	44.67	Lys[48]	122.50	7.95	54.46	34.40	121.81	7.69	53.84
Lys[11]	122.50	7.24	56.20	33.31	123.64	7.28	55.98	Gln[49]	123.51	8.59	55.82	28.96	122.41	8.56	55.44
Thr[12]	121.12	8.58	62.25	29.89	121.33	8.51	61.91	Leu[50]	126.41	8.52	54.08	41.38	nd	nd	53.60
Ile[13]	128.38	9.51	59.97	40.76	131.31	9.72	59.85	Glu[51]	123.75	8.32	56.11	31.75	123.82	8.32	55.57
Thr[14]	122.32	8.68	62.05	29.74	124.60	8.75	62.03	Asp[52]	120.79	8.05	56.49	40.76	120.92	8.08	56.32
Leu[15]	125.79	8.71	52.72	46.66	125.87	8.60	52.31	Gly[53]	108.19	9.50	45.15		107.05	9.23	44.77
Glu[16]	123.22	8.09	54.83	29.74	122.99	8.04	54.38	Arg[54]	119.77	7.36	54.31	32.38	119.96	7.38	54.05
Val[17]	118.28	8.89	58.45	36.26	118.20	8.89	58.11	Thr[55]	109.67	8.81	59.86	32.53	109.59	8.74	59.46
Glu[18]	119.48	8.59	53.69	32.07	119.38	8.56	53.29	Leu[56]	118.85	8.15	58.69	40.03	118.78	8.12	58.25
Ser[19]	118.52	9.21	62.49	67.01	118.46	9.18	61.70	Ser[57]	113.81	8.24	60.86	62.51	113.81	8.20	60.52
Ser[20]	109.40	7.26	57.23	63.44	109.43	7.23	56.89	Asp[58]	124.76	7.87	57.27	40.14	124.91	7.86	56.85
Asp[21]	124.01	7.82	55.66	40.76	124.12	7.79	55.26	Tyr[59]	116.30	7.20	58.06	40.05	116.41	7.16	57.71
Thr[22]	109.08	7.94	59.60	31.75	109.28	7.90	59.23	Asn[60]	116.82	8.11	54.06	37.35	116.84	8.07	53.71
Ile[23]	122.00	8.68	62.18	34.86	122.17	8.56	61.81	Ile[61]	119.31	7.20	62.35	36.57	119.66	7.25	61.92
Asp[24]	118.79	9.43	57.03	39.77	119.40	9.30	56.64	Gln[62]	125.76	7.61	53.53	31.60	125.75	7.60	53.17
Asn[25]	120.23	7.99	56.00	38.59	120.24	7.98	55.58	Lys[63]	121.23	8.42	57.91	32.53	121.12	8.36	57.41
Val[26]	122.70	8.08	67.69	30.67	122.77	8.08	67.21	Glu[64]	115.40	9.26	nd	65.61	115.70	9.18	57.82
Lys[27]	119.51	8.53	59.31	33.46	119.50	8.44	58.79	Ser[65]	115.57	7.62	60.78	64.84	115.67	7.63	60.43
Ser[28]	118.04	8.10	62.39	67.17	117.88	8.10	61.92	Thr[66]	118.09	8.67	62.37	30.51	118.15	8.65	61.91
Lys[29]	123.74	7.93	59.72	33.15	124.12	7.95	59.31	Leu[67]	128.39	9.37	53.70	44.18	128.50	9.38	53.39
Ile[30]	121.78	8.29	65.97	36.77	122.48	8.22	65.81	His[68]	120.04	9.20	55.86	31.91	119.07	8.94	55.75
Gln[31]	124.23	8.48	60.01	67.32	124.32	8.43	59.46	Leu[69]	124.70	8.27	53.69	44.18	125.10	8.47	53.25
Asp[32]	120.53	8.04	57.29	40.76	121.09	8.23	56.90	Val[70]	127.41	9.14	60.54	34.71	127.92	9.24	nd
Lys[33]	116.34	7.42	58.14	34.09	116.55	7.47	57.93	Leu[71]	123.88	8.07	53.90	42.78	nd	nd	nd
Glu[34]	115.01	8.70	55.24	33.15	113.73	8.56	54.56	Arg[72]	124.27	8.55	55.61	31.13	nd	nd	nd
Gly[35]	109.45	8.48	45.95		109.74	8.48	45.53	Leu[73]	124.99	8.29	54.76	42.32	nd	nd	nd
Ile[36]	120.94	6.14	57.72	40.45	121.13	6.12	57.31	Arg[74]	122.50	8.36	56.39	30.67	nd	nd	nd
Pro[37]	nd		nd	nd	nd		nd	Gly[75]	111.62	8.42	45.14		nd	nd	nd
Pro[38]	nd		66.04	32.53	nd		65.48	Gly[76]	115.74	7.89	45.98		nd	nd	nd

[a] Not determined.

Fourier electron density maps from X-ray analyses (*42*). Therefore, we will discuss the interaction between yeast ubiquitin and YUH1 on the basis of the coordinates of human ubiquitin (PDB accession code 1UBI), although the coordinates of yeast ubiquitin have not been deposited.

YUH1 was titrated into a sample of uniformly ^{15}N-labeled ubiquitin. The titration of the YUH1 perturbed some of the amide ^{1}H and ^{15}N chemical shifts of the ubiquitin residues. The titration was continued until the addition of YUH1 caused no further changes in the spectra. By carrying out such titrations, it is usually a simple matter to follow the changes in the positions of individual cross-peaks. Thus, the amide resonances of ubiquitin upon binding with YUH1 were mainly assigned using this procedure. Furthermore, the assignments were confirmed through analyses of the HNCA and HN(CO)CA spectra of the complex (Table 1). The $^{1}H-^{15}N$ HSQC spectrum of ubiquitin in the presence of YUH1, with the amide resonance assignments, is shown in Figure 2b.

Amide ^{1}H and ^{15}N Chemical Shift Changes of Ubiquitin upon YUH1 Binding. Panels a and c of Figure 3 depict the amide ^{1}H and ^{15}N chemical shift changes upon binding with YUH1 in the $^{1}H-^{15}N$ HSQC spectra as a function of the position in the ubiquitin sequence, respectively. For the sake of clarity in observing the regions where the chemical shifts have changed, the weighted sum of the chemical shift changes of both nuclei for all residues is shown in Figure 3c. The weighted sum was calculated on the ratio of the gyromagnetic ratios for protons and for nitrogens (9.87) (*43*), indicating the overall effects on each individual amide NH group. This ratio is in agreement with the ratio of the backbone amide chemical shift dispersions in the nitrogen and proton dimensions (8.92) of the yeast ubiquitin obtained in this study. Complex formation induced not only chemical shift changes but also line broadening of the signals as well. The extreme line broadening resulted in the disappearance of signals. Thus, the chemical shift changes for some residues could not be determined because of the disappearance of signals (indicated by *). It is interesting that many amide resonances of ubiquitin were affected to some degree by binding to YUH1.

Assessment of Complexation-Induced Chemical Shift Perturbations. To ascertain whether all portions of ubiquitin forms complex with YUH1 under the NMR condition, we determined the K_d value of the complex by using IAsys. The K_d value was 18.7 ± 1.7 μM, which indicates that ubiquitin and YUH1 form a rather stable complex and that almost all portions of ubiquitin are in complex with YUH1 under the NMR condition (2 and 2.2 mM, respectively). We also measured $^{1}H-^{15}N$ HSQC spectra when an excess amount of YUH1 was added to the ubiquitin−YUH1 complex, where the final concentration of ubiquitin and YUH1 is 2 and 4 mM, respectively. No more chemical shift changes of NH resonances of ubiquitin were observed compared with the

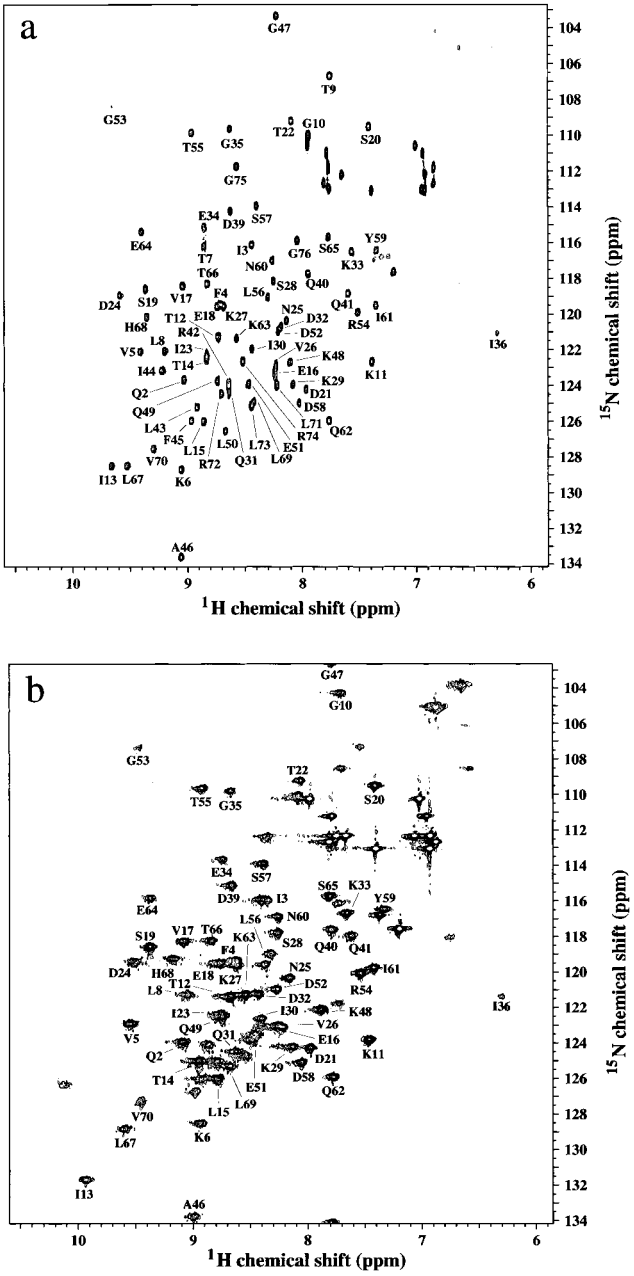

FIGURE 2: ^{1}H−^{15}N HSQC spectra of ^{15}N-enriched ubiquitin in the absence (panel a) and the presence (panel b) of YUH1. All of the backbone amide resonances observable in these spectra were assigned and are labeled with the one-letter representation and the residue number.

spectra of the 1:1.1 complex. Therefore, we concluded that such chemical shift changes may be used to map the interaction regions of the ubiquitin−YUH1 complex. Indeed, a number of workers have used complexation-induced shifts in ^{1}H−^{15}N HSQC spectra to map the intermolecular interaction regions of protein−protein complexes (*43*−*49*). In most cases, cutoffs of more than 0.2 ppm and more than 0.02 (or more than 0.04) ppm for ^{15}N and ^{1}H chemical shift changes, respectively, were used to distinguish between affected and unaffected resonances. Using these criteria, approximately 75% of the ubiquitin residues would be affected by YUH1 binding. It is unlikely that such a large number of residues are directly involved in YUH1 binding. Therefore, it is necessary to consider the origins of the individual chemical shift perturbations to delineate the interacting region.

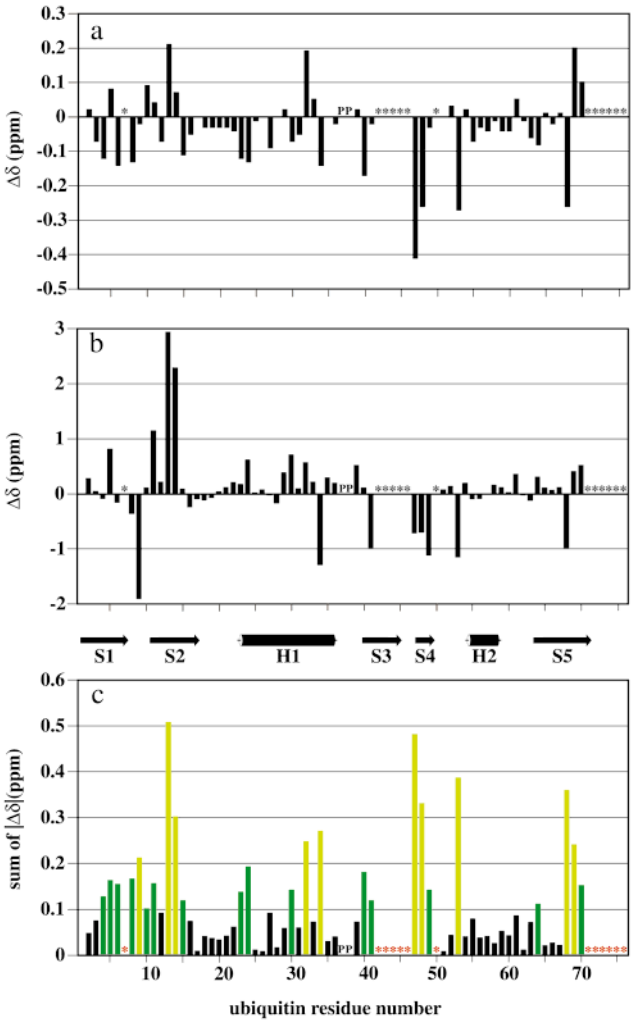

FIGURE 3: Chemical shift perturbations of backbone amide protons (panel a) and nitrogens (panel b) caused by YUH1 binding. The weighted sum of the total chemical shift perturbations for both nuclei (panel c) (see Materials and Methods for details). Residues are colored light green if their weighted sum of $|\Delta\delta|$ is larger than 0.2 ppm and dark green if their weighted sum of $|\Delta\delta|$ is 0.1−0.2 ppm. The residues that could not be clearly assigned, due to the disappearance of the signals, are indicated by asterisks colored red.

When two proteins form a complex, various interactions between them will inevitably cause changes in the environments of the nuclei in the amino acid residues at the interface, resulting in chemical shift changes. Moreover, conformational changes upon complex formation can also contribute to chemical shift perturbations. Many perturbations may arise from changes in the chemical environments of NH groups not located at, but close to, the interface. It is noteworthy that even a minor conformational change, for example, of an aromatic ring, or of the donor and acceptor in a hydrogen bond, can lead to a substantial shift. Thus, great care must be taken to assess the complexation-induced chemical shift perturbations. Indeed, Spitzfaden et al. have shown that although perturbed resonances give good initial estimates of a binding surface, the effects extend beyond the direct contact area (*50*).

Figure 3c shows the perturbations classified into four categories (the disappearance of signals and the small, intermediate, and large changes in chemical shifts). The disappearance of signals category contains residues with

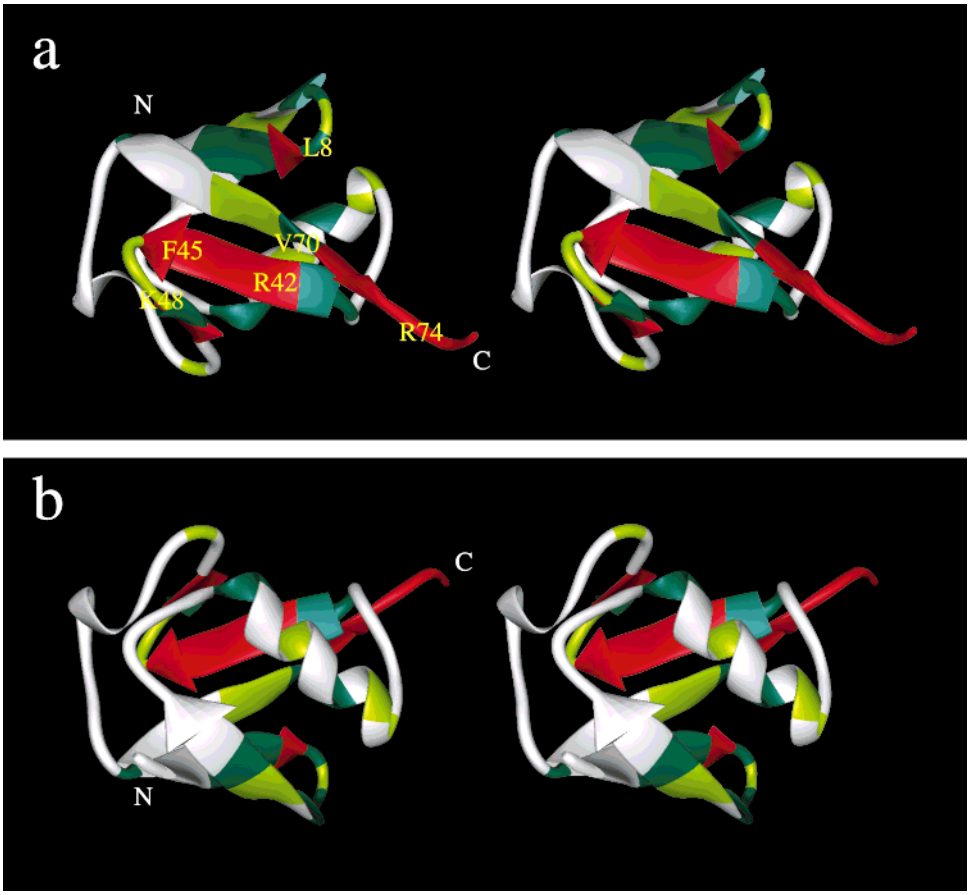

FIGURE 4: Mapping of the chemical shift changes on the 3D structure of ubiquitin. (Panel a) Stereopair ribbon diagram of ubiquitin. Residues are colored light green if their weighted sum of $|\Delta\delta|$ is larger than 0.2 ppm and dark green if their weighted sum of $|\Delta\delta|$ is 0.1−0.2 ppm. The residues that could not be clearly assigned, due to the disappearance of the signals, are colored red. (Panel b) Stereopair of the same ribbon diagram as in (a), obtained by a 180° rotation about the horizontal axis of the stereopair (a). These figures were drawn using MIDAS Plus (*62*).

chemical shifts that could not be assigned, due to the disappearance of the signals (red). The large changes in chemical shift category contains residues with sums of chemical shift changes between 0.2 and 0.6 ppm (light green), the intermediate changes category contains residues with changes between 0.1 and 0.2 ppm (dark green), and the small changes category contains the remaining perturbed residue with changes smaller than 0.1 ppm (black). Approximately 20% of the amide resonances of ubiquitin belong to the disappearance of signals category, approximately 10% of the amide resonances of ubiquitin belong to the large changes category, and approximately 20% of the amide resonances of ubiquitin belong to the intermediate changes category. The disappearance of signals and large changes categories used in this study are analogous to the cutoffs applied by other workers to determine interprotein contact residues (*43*−*49*). Residues belonging to these categories are likely to be involved in direct interactions with YUH1.

Mapping of the Chemical Shift Changes on the 3D Structure of Ubiquitin. According to the categories described above, 39 residues were selected: 13 in the disappearance of signals category (residues 7, 42−46, 50, and 71−76), 10 in the large changes category (residues 9, 13, 14, 32, 34, 47, 48, 53, 68, and 69), and 15 in the intermediate changes category (residues 4−6, 8, 10, 11, 15, 23, 24, 30, 40, 41, 49, 64, and 70). Thus, we mapped these perturbed residues on the 3D structure of ubiquitin determined previously (*42*, *51*−*53*). The positions of these residues in the 3D structure of ubiquitin are shown in Figure 4, with residues in the disappearance category colored red, those in the large changes category colored light green, and those in the intermediate changes category colored dark green. Ubiquitin consists of a five-stranded β-sheet and one long (residues 23−34) and one short (residues 56−59) α-helix. The C-terminus of ubiquitin follows the last (fifth) β-strand. In this structure, the residues in the disappearance and large changes categories are dispersed over a wide area on the C-terminus and the five-stranded β-sheet. However, the chemical shift changes of the amide resonances are small in the residues of the long α-helix (residues 23−34), which is located toward one side of the β-sheet. These observations suggest that YUH1 contacts ubiquitin through the surface of the β-sheet opposite to the α-helix and recognizes ubiquitin through not only the C-terminus but also the wide area in the vicinity of the C-terminus. In contrast to the members of the papain superfamily, which exhibit broad substrate specificity (*54*), YUH1 shows strict specificity to the C-terminus of ubiquitin. The facts that about 30% of the ubiquitin residues are involved in interactions with YUH1 and that these residues are distributed along a wide area are consistent with the high substrate specificity of YUH1.

On the basis of the crystal structure of UCH-L3, Johnston et al. proposed a model for ubiquitin binding to UCH-L3 (*18*). The model described a deep S′ site substrate cleft

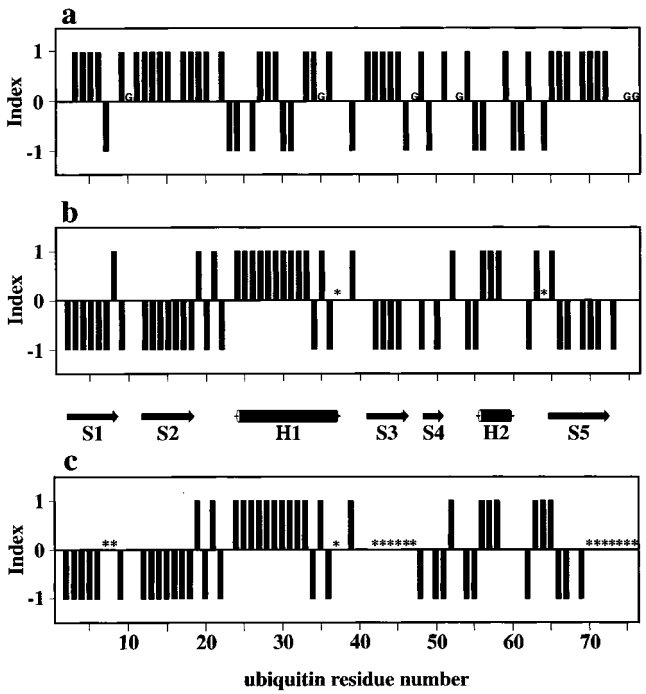

FIGURE 5: Chemical shift indices of the $^{13}C^{\alpha}$ (panels b and c) and $^{13}C^{\beta}$ (panel a) resonances for ubiquitin in the absence (panels a and b) and the presence (panel c) of YUH1. The chemical shift indices of the $C^{\alpha}H$ resonances are indicated by ternary indices, with values of −1, 0, and 1 (*63*). The residues that could not be clearly assigned and the glycine residues are indicated by asterisks and "G", respectively.

formed in UCH-L3 by a conformational change upon binding to ubiquitin, because the UCH-L3 crystal structure lacks a groove of S′ sites. Kinetic and thermodynamic studies indicated that UCH-L3 is able to utilize the free energy released from its extensive interaction with ubiquitin for the conformational change and the stabilization of the catalytic transition state (*55*). Furthermore, UCH-L3 has 60% amino acid sequence homology as compared with YUH1. Taken together, it is thought that the ubiquitin recognition mechanisms of YUH1 and UCH-L3 are similar in both cases. Thus, the broad range of interactions between YUH1 and ubiquitin suggested by our results may possibly reflect a conformational change in YUH1, similar to that of UCH-L3.

Recognition of Ubiquitin Residues by YUH1. It is noteworthy that the amide resonances of the basic residues (Arg42, Arg72, and Lys74) were highly perturbed. In the crystal structure of ubiquitin, these basic residues are exposed at the protein surface (*42*, *51*−*53*) (Figure 5). These positively charged basic residues may be involved in direct interactions with the negatively charged acidic residues on YUH1. In fact, the molecular surface of YUH1 seems to be abundant with negatively charged residues, based on the fact that YUH1 binds to DEAE Sephacel even at higher salt concentrations of (see Materials and Methods). In addition to the positively charged area, hydrophobic residues on ubiquitin (Leu8, Ile44, Phe45, Val70, Leu71, and Leu73) are also likely to contribute to the YUH1 binding. Among the hydrophobic residues in ubiquitin, Leu8 and Val70 are in the intermediate changes category in the chemical shift perturbation experiment, and Ile44, Phe45, Leu71, and Leu73 are in either the disappearance or the large changes category.

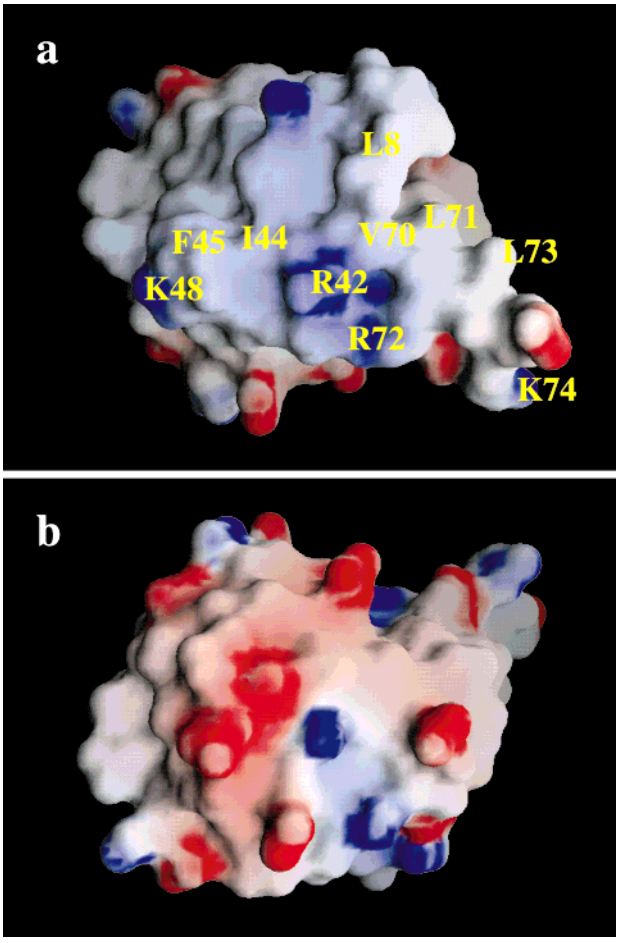

FIGURE 6: Electrostatic potential representations of ubiquitin. Blue regions represent positive potentials of lysine residues. White regions represent neutral potentials. This figure was prepared using the program GRASP (*64*). Panels a and b are in the same orientations as the stereopairs in panels a and b of Figure 4, respectively.

Although Leu8 and Val70 are in the intermediate changes category, these two residues are likely to contribute to the hydrophobic interaction with YUH1. This is because Leu8 and Val70 are exposed at the protein surface (*42*, *51*−*53*), and the residues adjacent to Leu8 and Val70 (Thr7, Thr9, Leu69, and Leu71) have highly perturbed chemical shifts of their amide resonances. Interestingly, the amide resonances of Ile13, Leu43, Leu50, and Leu69, the side chains of which are found within a hydrophobic core and not on the surface, were also highly perturbed.

Although many amide resonances of ubiquitin were highly perturbed upon binding with YUH1, the conformation of ubiquitin does not seem to be largely changed upon binding with YUH1. Figure 5 shows the chemical shift indices (CSIs) of the $^{13}C^{\alpha}$ (panels b and c) and $^{13}C^{\beta}$ (panel a) resonances for ubiquitin in the absence (panels a and b) and the presence (panel c) of YUH1, respectively. These data show that both CSIs of ubiquitin in the absence and presence of YUH1 are similar to each other, suggesting that the conformation of ubiquitin is not largely changed upon binding with YUH1. Therefore, most of the amide resonances of ubiquitin that are highly perturbed upon binding with YUH1 may be attributed to the interaction of the residues with YUH1.

A recent study on the substrate specificity of UCH-L3, which shares 30% amino acid sequence identity with YUH1,

suggested that UCH-L3 catalyzes the removal of the lysine residue from the C-terminus of Lys48-linked diubiquitin (Ub-^{K48}Ub) (*21*). Since both N^{ϵ}-Ub-[L-lysine] and N^{α}-(Ub-^{K48}-Ub)-[L-lysine] are good substrates for UCH-L3, while Ub-^{K48}Ub is not, Lys48 is not thought to be recognized by UCH-L3. In the case of ubiquitin isopeptidase in the PA700 regulatory complex, which belongs to the UBP family and trims the polyubiquitin chains by releasing one subunit from the proximal end of the chain, the specificity determinants include Leu8, Ile44, and Lys48 on the distal ubiquitin (*56*). In our NMR study, the chemical shift of Lys48 was highly perturbed. Thus, there are two possibilities for the cause of the chemical shift perturbation of Lys48. One possibility is that the chemical shift perturbation of Lys48 is due to the conformational change of ubiquitin, and the other is that the P1 specificity of YUH1 is slightly different from that of UCH-L3 and similar to that of the PA700 isopeptidase. (Substrate residues amino- and carboxyl-terminal proximal to the scissile bond are designated as P and P′, respectively, and the corresponding binding sites on the enzyme are designated as S and S′ (*57*).]

Comparison of the Recognition Mechanism of the Substrates of YUH1 with Other Cysteine Proteases. YUH1 is a cysteine protease, and studies on UCH-L3 (human homologue of YUH1) have suggested a structural similarity to the papain family of cysteine proteases (*18*). The substrate specificities of papain, cathepsin, and glycyl endopeptidase, which belong to the papain family, have been well studied. Papain has a large active site that extends over about 25 Å and can be divided into seven subsites, S4−S3′ (*57*). However, the substrate specificity of papain is rather low, and it can cleave substrates as small as dipeptides (*58*). The cysteine class of cathepsins has been classified into four subtypes: B, H, L, and S. Cathepsins also show low substrate specificity, as indicated by the cleavage analysis of the insulin B chain (*59*). Among the papain family of cysteine proteases, only glycyl endopeptidase shows rather high substrate specificity. Glycyl endopeptidase cleaves peptide bonds primarily after glycine residues. However, the P2−P4 residues are not conserved for the substrates of this enzyme (*60*). In contrast to such low substrate specificities of the other cysteine proteases, YUH1 shows high substrate specificity. The sequence of P5−P1, which corresponds to the C-terminus of ubiquitin, is RLRGG. YUH1 does not seem to recognize the P1′ amino acid, as YUH1 can cleave many kinds of C-terminal adducts, with the exception of a P1′ proline (*17*). However, YUH1 strictly recognizes the C-terminus of ubiquitin. Furthermore, YUH1 not only recognizes a single polypeptide chain of the sequence with P5−P1 (RLRGG) of the C-terminus of ubiquitin but also recognizes the wide area maintained by the tertiary structure of the substrate ubiquitin. This is supported by the fact that YUH1 does not cleave the peptide bonds even if a substrate, other than ubiquitin, possesses the same amino acid residues P1−P4 as in ubiquitin (Kohno et al., unpublished data). This suggestion is consistent with our present data, which show that the chemical shifts of the amide resonances in a wide area of ubiquitin are perturbed upon YUH1 binding. This is the first example of a novel protease recognition mechanism, wherein the protease recognizes the overall tertiary structure of the substrate in addition to the cleavage site.

Thus, YUH1 possesses novel substrate recognition for a protease, in that it also recognizes the tertiary structure of the substrate ubiquitin. The information obtained in this study may help in the structure-based design of mutant YUH1 proteins, which can cleave different substrates than ubiquitin extensions. Furthermore, this study provides a structural basis for understanding the mechanisms of diseases caused by mutations of UCH proteases.

ACKNOWLEDGMENT

We are grateful to Dr. Judyth Sassoon for a critical reading of the manuscript. We also express our gratitude to Dr. Koji Takio for his help in the measurement on the DRX600 spectrometer in the Division of Biomolecular Characterization, RIKEN.

REFERENCES

1. Ciechanover, A., and Schwartz, A. L. (1994) *FASEB J. 8*, 182−191.
2. Hershko, A., and Ciechanover, A. (1992) *Annu. Rev. Biochem. 61*, 761−807.
3. Jentsch, S. (1992) *Trends Cell. Biol. 2*, 98−103.
4. Wilkinson, K. D., Tashayev, V. L., O'Connor, L. B., Larsen, C. N., Kasperek, E., and Pickart, C. M. (1995) *Biochemistry 34*, 14535−14546.
5. Chau, V., Tobias, J. W., Bachmair, A., Marriott, D., Ecker, D. J., Gonda, D. K., and Varshavsky, A. (1989) *Science 243*, 1576−1583.
6. Gregori, L., Poosch, M. S., Cousins, G., and Chau, V. (1990) *J. Biol. Chem. 265*, 8354−8357.
7. Wilkinson, K. D. (1997) *FASEB J. 11*, 1245−1256.
8. Ozkaynak, E., Finley, D., Solomon, M. J., and Varshavsky, A. (1987) *EMBO J. 6*, 1429−1439.
9. Tobias, J. W., and Varshavsky, A. (1991) *J. Biol. Chem. 266*, 12021−12028.
10. Baker, R. T., Tobias, J. W., and Varshavsky, A. (1992) *J. Biol. Chem. 267*, 23364−23375.
11. Pickart, C. M., and Rose, I. A. (1985) *J. Biol. Chem. 260*, 7903−7910.
12. Papa, F. R., and Hochstrasser, M. (1993) *Nature 366*, 313−319.
13. Huang, Y., Baker, R. T., and Fischer-Vize, J. A. (1995) *Science 270*, 1828−1831.
14. Henchoz, S., De Rubertis, F., Pauli, D., and Spierer, P. (1996) *Mol. Cell. Biol. 16*, 5717−5725.
15. Moazed, D., and Johnson, D. (1996) *Cell 86*, 667−677.
16. Zhu, Y., Carroll, M., Papa, F. R., Hochstrasser, M., and D'Andrea, A. D. (1996) *Proc. Natl. Acad. Sci. U.S.A. 93*, 3275−3279.
17. Miller, H. I., Henzel, W. J., Ridgmay, J. B., Kuang, W.-J., Chisholm, V., and Liu, C.-C. (1989) *Biotechnology 7*, 698−704.
18. Johnston, S. C., Larsen, C. N., Cook, W. J., Wilkinson, K. D., and Hill, C. P. (1997) *EMBO J. 16*, 3787−3796.
19. Roff, M., Thompson, J., Rodriguez, M. S., Jacque, J. M., Baleux, F., Arenzana-Seisdedos, F., and Hay, R. T. (1996) *J. Biol. Chem. 271*, 7844−7850.
20. Wilkinson, K. D., Cox, M. J., Mayer, A. N., and Frey, T. (1986) *Biochemistry 25*, 6644−6649.
21. Larsen, C. N., Krantz, B. A., and Wilkinson, K. D. (1998) *Biochemistry 37*, 3358−3368.
22. Kusunoki, H., Wakamatsu, K., Sato, K., Miyazawa, T., and Kohno, T. (1998) *Biochemistry 37*, 4782−4790.
23. Kohno, T., Kusunoki, H., Sato, K., and Wakamatsu, K. (1998) *J. Biomol. NMR 12*, 109−121.
24. Larsen, C. N., Price, J. S., and Wilkinson, K. D. (1996) *Biochemistry 35*, 6735−6744.
25. Mori, H., Yano, T., Kobayashi, T., and Shimizu, S. (1979) *J. Chem. Eng. Jpn. 12*, 313−319.

26. Mizutani, S., Mori, H., Shimazu, S., Sakaguchi, K., and Kobayashi, T. (1986) *Biotechnol. Bioeng. 28*, 204−209.
27. Grzesiek, S., and Bax, A. (1992) *J. Magn. Reson. 96*, 432−440.
28. Kay, L. E., Ikura, M., Tschudin, R., and Bax, A. (1990) *J. Magn. Reson. 89*, 496−514.
29. Muhandiram, D. R., and Kay, L. E. (1994) *J. Magn. Reson. B 103*, 203−216.
30. Wittekind, M., and Mueller, L. (1993) *J. Magn. Reson. B 101*, 201−205.
31. Yamazaki, T., Lee, W., Revington, M., Mattiello, D. L., Dahlquist, F. W., Arrowsmith, C. H., and Kay, L. E. (1994) *J. Am. Chem. Soc. 116*, 6464−6465.
32. Yamazaki, T., Lee, W., Arrowsmith, C. H., Muhandiram, D. R., and Kay, L. E. (1994) *J. Am. Chem. Soc. 116*, 11655−11666.
33. Piotto, M., Saudek, V., and Sklenar, V. (1992) *J. Biomol. NMR 2*, 661−665.
34. Grzesiek, S., and Bax, A. (1993) *J. Am. Chem. Soc. 115*, 12539−12594.
35. Delaglio, F., Grzesiek, S., Vuister, G. W., Zhu, G., Pfeifer, J., and Bax, A. (1995) *J. Biomol. NMR 6*, 277−923.
36. Zhu, G., and Bax, A. (1992) *J. Magn. Reson. 100*, 202−207.
37. Zhu, G., and Bax, A. (1990) *J. Magn. Reson. 90*, 405−410.
38. Kraulis, P. J. (1989) *J. Magn. Reson. 24*, 627−633.
39. Kraulis, P. J., Domaille, P. J., Campbell-Burk, S. L., Van Aken, T., and Laue, E. D. (1994) *Biochemistry 33*, 3515−3531.
40. Wishart, D. S., Bigam, C. G., Yao, J., Abildgaard, F., Dyson, H. J., Oldfield, E., Markley, J. L., and Sykes, B. D. (1995) *J. Biomol. NMR 6*, 135−140.
41. Stockman, B. J., Euvrard, A., and Scahill, T. A. (1993) *J. Biomol. NMR 3*, 285−296.
42. Vijay-Kumar, S., Bugg, C. E., Wilkinson, K. D., Vierstra, R. D., Hatfield, P. M., and Cook, W. J. (1987) *J. Biol. Chem. 262*, 6396−6399.
43. Zhao, Q., Abeygunawardana, C., and Mildvan, A. S. (1997) *Biochemistry 36*, 3458−3472.
44. Osborne, M. J., Wallis, R., Leung, K. Y., Williams, G., Lian, L. Y., James, R., Kleanthous, C., and Moore, G. R. (1997) *Biochem. J. 323*, 823−831.
45. Chen, Y., Reizer, J., Saier, M. H., Jr., Fairbrother, W. J., and Wright, P. E. (1993) *Biochemistry 32*, 32−37.
46. Jones, D. N., Bycroft, M., Lubienski, M. J., and Fersht, A. R. (1993) *FEBS Lett. 331*, 165−172.
47. Clubb, R. T., Omichinski, J. G., Clore, G. M., and Gronenborn, A. M. (1994) *FEBS Lett. 338*, 93−97.
48. Gunther, U. L., Liu, Y., Sanford, D., Bachovchin, W. W., and Schaffhausen, B. (1996) *Biochemistry 35*, 15570−15581.
49. Williamson, R. A., Carr, M. D., Frenkiel, T. A., Feeney, J., and Freedman, R. B. (1997) *Biochemistry 36*, 13882−13889.
50. Spitzfaden, C., Weber, H. P., Braun, W., Kallen, J., Wider, G., Widmer, H., Walkinshaw, M. D., and Wuthrich, K. (1992) *FEBS Lett. 300*, 291−300.
51. Vijay-Kumar, S., Bugg, C. E., and Cook, W. J. (1987) *J. Mol. Biol. 194*, 531−544.
52. Di Stefano, D. L., and Wand, A. J. (1987) *Biochemistry 26*, 7272−7281.
53. Weber, P. L., Brown, S. C., and Mueller, L. (1987) *Biochemistry 26*, 7282−7290.
54. Fox, T., Mason, P., Storer, A. C., and Mort, J. S. (1995) *Protein Eng. 8*, 53−57.
55. Dang, L. C., Melandri, F. D., and Stein, R. L. (1998) *Biochemistry 37*, 1868−1879.
56. Lam, Y. A., DeMartino, G. N., Pickart, C. M., and Cohen, R. E. (1997) *J. Biol. Chem. 272*, 28438−28446.
57. Schechter, I., and Berger, A. (1967) *Biochem. Biophys. Res. Commun. 27*, 157−162.
58. Duan, Y., and Laursen, R. A. (1994) *Anal. Biochem. 216*, 431−438.
59. Barrett, A. J., and Kirschke, H. (1981) *Methods Enzymol. 80*, 535−561.
60. Rawlings, N. D., and Barrett, A. J. (1994) *Methods Enzymol. 244*, 461−486.
61. Barton, G. L. (1993) *Protein Eng. 6*, 37−40.
62. Ferrin, T. E., Huang, C. C., Jarvis, L. E., and Langridge, R. (1988) *J. Mol. Graphics 6*, 13−27.
63. Wishart, D. S., and Sykes, B. (1994) *J. Biomol. NMR 4*, 171−180.
64. Nicholls, A., Sharp, K. A., and Honig, B. (1991) *Proteins: Struct., Funct., Genet. 11*, 281−296.

BI990310Y